

Extended fractional-order Jeffreys model of viscoelastic hydraulic cylinder

Michael Ruderman

University of Agder, 4604-Norway

Abstract

Novel modeling approach for viscoelastic hydraulic cylinders with negligible inertial forces is proposed based on the extended fractional-order Jeffreys model. Analysis and physical reasoning for the parameter constraints and order of the fractional derivatives are provided. The comparison between the measured and computed frequency response functions and time domain transient response argue in favor of the proposed four-parameters fractional-order model.

Keywords: Fractional-order dynamics, viscoelasticity, dashpots, Jeffreys model, hydraulic actuators

1. Introduction

In viscoelasticity, the fractional-order models established, since long, as more accurate and flexible, while being with lower dimension of the parameters space, than their integer-order counterparts. Analysis of various properties of the viscoelastic behavior such as creep, relaxation, viscosity, and initial conditions can be found e.g. in [1, 2]. It is also worth to recall that one of the widespread formulations of the differential-order operator, namely Caputo, has been elaborated in context of a viscoelastic stress-strain relation and memory mechanism associated with the initial conditions, see e.g. [3] for details.

Not only viscoelastic solids have benefited from the fractional-order modeling. Also soft biological tissues have been experimentally studied and identified by means of fractional calculus in viscoelasticity [4]; more recent review of the fractional calculus in modeling biological phenomena can be found in [5]. Other examples of complex impact and retardation dynamics, approached with help of the fractional-order modeling, can be found when analyzing e.g. backlash [6] or piezoelectric creep [7]. Fractional-order modeling has been shown as efficient and also identified with experiments when describing transient behavior of super-capacitors [8]. Besides the above mentioned examples, significant efforts in the fractional-order calculus of dynamic systems should be credited to the fractional-order controllers, though not directly related to the recent study. For overviews on the tuning of fractional-order controllers for industry applications and fractional PID controllers we exemplarily refer to [9] and [10] respectively.

In this brief, we make use of the fractional-order viscoelastic behavior to describe the principal dynamics of the standard dashpot-type hydraulic cylinders by a low-parameters and -order model, with yet accurate prediction

of the frequency response characteristics. The proposed solution is approaching the Jeffreys [11] viscoelastic model, though extending it by an additional stiffness, generalizing to the fractional derivatives, and setting physically reasonable constraints on the parameters and differential-order. While providing all necessary preliminaries of the fractional-order calculus (see Section 2), for the basics on applied hydraulics we refer to [12]. Then the main contribution of the paper is in Section 3, and the experimental evaluation and discussion are provided in Section 4.

2. Fractional differentiation

In approach to the seminal literature on the fractional-order calculus e.g. [13, 14, 15], we will use a fractional α -order operator on the a and t limits, defined by

$${}_a D_t^\alpha = \begin{cases} \frac{d^\alpha}{dt^\alpha} & \text{for } \alpha > 0, \\ 1 & \text{for } \alpha = 0, \\ \int_a^t dt^{-\alpha} & \text{for } \alpha < 0. \end{cases} \quad (1)$$

For the sake of practical relevance we confine ourselves to the real fractional orders, i.e. $\alpha \in \mathbb{R}$, often denoted as a *non-integer* differentiation, correspondingly integration. For the same reasoning of the practical (engineering) applications we will consider zero initial time i.e. $a = 0$.

The classical definition of Riemann-Liouville α -derivative of a continuous function $f(t)$, with $n-1 \leq \alpha < n$ where n is an integer, is given by

$${}_0 D_t^\alpha f(t) = \frac{1}{\Gamma(n-\alpha)} \frac{d^n}{dt^n} \int_0^t \frac{f(\tau)}{(t-\tau)^{\alpha-n+1}} d\tau. \quad (2)$$

Here $\Gamma(\cdot)$ is the Gamma function. We should notice that solving differential equations in terms of the Riemann-Liouville derivatives (2) requires the initial conditions

$$[{}_0 D_t^{\alpha-k} f(t)]_{t \rightarrow 0} = c_k \quad \text{for } k = 1, 2, \dots, n \quad (3)$$

Email address: michael.ruderman@uia.no (Michael Ruderman)

to be known, correspondingly determined. That is one needs the initial values of the $(\alpha - k)$ -fractional derivatives of the function $f(t)$. This is particularly visible when considering the Laplace transform $F(s) = \mathcal{L}\{f(t)\}$ of the Riemann-Liouville fractional derivative, cf. [15], given by

$$\mathcal{L}\{ {}_0D_t^\alpha f(t) \} = s^\alpha F(s) - \sum_{k=0}^{n-1} s^k [{}_0D_t^{\alpha-k-1} f(t)]_{t=0}. \quad (4)$$

The Grünwald-Letnikov definition, cf. [15],

$${}_0D_t^\alpha f(t) = \lim_{h \rightarrow 0} h^{-\alpha} \sum_{i=0}^{[th^{-1}]} (-1)^i \binom{\alpha}{i} f(t - ih) \quad (5)$$

of the fractional-order derivative is valid for any $\alpha \in \mathbb{R}$ and is particularly suitable for numerical implementations, since it constitutes the limit of the difference quotient

$$\Delta_h^\alpha f(t) \approx {}_0D_t^\alpha f(t), \quad (6)$$

with the time step $h \rightarrow 0$. In (5), the operator $[x]$ means the integer part of x , while i is the index of the discrete time series of t . The binomial coefficients, which are sign alternating and summarized as

$$w_i^{(\alpha)} = (-1)^i \binom{\alpha}{i} \quad \text{for } i = 0, 1, 2, \dots, \quad (7)$$

can be evaluated recursively, cf. [15], by

$$w_0^{(\alpha)} = 1; \quad w_i^{(\alpha)} = \left(1 - \frac{\alpha + 1}{i}\right) w_{i-1}^{(\alpha)} \quad \text{for } i = 1, 2, 3, \dots \quad (8)$$

Further we will also make use of the fact that for zero initial conditions the Laplace transform is given by

$$\mathcal{L}_0\{ {}_0D_t^\alpha f(t) \} = s^\alpha F(s), \quad (9)$$

and will write the Fourier transform as

$$\mathcal{F}\{ {}_0D_t^\alpha f(t) \} = (j\omega)^\alpha F(\omega). \quad (10)$$

Note that for \mathcal{F} the magnitude and phase responses are conventionally given as in the case of $\alpha \in \mathbb{Z}$.

3. Modeling

Our starting point is the standard dashpot element, used in viscoelasticity for modeling and analysis and representing an ideal linear viscous fluid. A constantly applied stress σ produces a constant strain rate so that

$$\sigma = \mu \frac{d}{dt} \varepsilon, \quad (11)$$

where μ is the coefficient of viscosity of a Newtonian fluid. Note that a linear dashpot, as basic mechanical element, is approaching a simple piston-cylinder, with one degree of freedom x , for which the stress equivalent to the hydraulic

pressure is substituted by the applied force τ . Correspondingly, the strain rate is equivalent to the rate of displacement, so that in the Laplace domain one obtains

$$x = \mu^{-1} s^{-1} \tau. \quad (12)$$

Obviously (12) constitutes a free integrator dynamics, this way yielding a simple first-order lumped model of the viscous driven motion when inertial effects are neglected. Note that the latter is justified for multiple hydraulic cylinders, deployed as the actuators, in which the viscoelastic forces largely dominate over the inertial.

Next we elaborate whether the hydraulic cylinder force, induced by the pressure difference, undergoes self the dynamic transients to be captured by a viscoelastic behavior. The stress-strain relation of the standard linear solid, also denoted as Zener, model is given by

$$E \left[\frac{1}{\phi} \frac{d}{dt} + 1 \right] \varepsilon(t) = \left[\frac{1}{\varphi} \frac{d}{dt} + 1 \right] \sigma(t), \quad (13)$$

where E is a suitable elastic modulus. The positive constants $\phi^{-1} > \varphi^{-1}$ refer to the retardation and relaxation times, see e.g. [11]. It can be noted that $\phi = \varphi$ simplifies (13) to a purely elastic material, i.e. $\sigma = E\varepsilon$, while (13) includes equally the Maxwell and Kelvin-Voigt models of the viscoelastic fluid, correspondingly solid, as limiting cases [3]. The otherwise unequal and non-zero time constants of retardation and relaxation shape the frequency characteristics of a standard linear solid within $\phi < \omega < \varphi$, while keeping it at different constant levels for $\omega \rightarrow 0$ and $\omega \rightarrow \infty$ limits. Since the dynamic behavior (13) has zero relative degree, its input-output transfer characteristics can also be considered as entirely unitless. For approaching a viscoelastic fluid in the closed hydraulic circuit (of cylinder) as a quasi-solid medium, the model (13) can be used for describing its dynamic compressibility. Thus, the applied stress σ appears in equivalence to the supplied pressure difference, while the strain ε mimics a stiff kinematic excitation, and therefore force, acting on the piston interface. In that equivalence, the elastic modulus appears as the bulk modulus [12] of hydraulic medium. The retardation time approaches the time constant of the effective force response to a stepwise change of the differential pressure. Similarly, the relaxation time relates to the time constant of the pressure response to an instantaneous change in the piston stroke and thus force on the piston interface.

3.1. Jeffreys model

The Jeffreys model [11] composes, essentially, the Kelvin-Voigt and dashpot elements connected in series, see structural arrangement in Figure 1. The overall strain (or relative displacement) rate is a superposition of both

$$\frac{d}{dt} \varepsilon = \frac{d}{dt} \varepsilon_1 + \frac{d}{dt} \varepsilon_2, \quad (14)$$

while the stress (correspondingly force) in both elements is the same, meaning

$$\sigma = K\varepsilon_1 + \mu_1 \frac{d}{dt} \varepsilon_1 = \mu_2 \frac{d}{dt} \varepsilon_2. \quad (15)$$

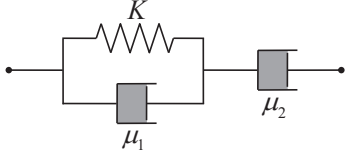


Figure 1: Jeffreys viscoelastic model.

Combining (14) and (15) and eliminating ε_1 and ε_2 results in the Jeffreys model of the form

$$\mu_2 \left[\frac{\mu_1}{K} \frac{d^2}{dt^2} + 1 \right] \varepsilon(t) = \left[\frac{\mu_1 + \mu_2}{K} \frac{d}{dt} + 1 \right] \sigma(t). \quad (16)$$

Here the relaxation and retardation times are given by $(\mu_1 + \mu_2)K^{-1}$ and $\mu_1 K^{-1}$ correspondingly. Note that, similar as in case of the Zener model, an elimination (set to zero) of μ_1 or μ_2 simplifies the Jeffreys model (16) to the Maxwell or Kelvin-Voigt model respectively.

3.2. Fractional-order formulation

Allowing for the fractional-order derivatives and considering the differential pressure and relative displacement input-output pair, the fractional-order Jeffreys model in the Laplace domain is written as

$$\mu s^\gamma (\lambda_2 s^\alpha + 1) x(s) = (\lambda_1 s^\beta + 1) \tau(s). \quad (17)$$

Note that a similar modified Jeffreys model has been also proposed, however for the viscoelastic fluids, in [16]. It is evident that for the same time constants $\lambda_1 = \lambda_2$ and fractional orders $\alpha = \beta$ the proposed model (17) reduces to the simple viscous dashpot, cf. with (12). While the general form (17) allows for all derivatives to be of the fractional-order, we will require $\gamma = 1$ for not violating causality and physical reasoning of the force-displacement transfer characteristics. This is analyzed below in context of the impulse response and its steady-state (final) value.

Unlike the original Jeffreys model cf. [11] and the modified one [16], the parameters inequality $\lambda_2 > \lambda_1$ is required for (17). Note that this implies the lag characteristics of the $x(s)/\tau(s)$ transfer function, which means a phase-lowering region and amplitude drop within $\lambda_1^{-1} < \omega < \lambda_2^{-1}$. From the structural viewpoint, it requires an additional spring that leads to a serial connection of the Zener model with the viscous dashpot (see above in Section 3). While the dynamics order and relative degree remain, this way, unchanged, the viscoelastic damping properties of the Zener model (13) argue in favor of the lag characteristics of (17). Indeed, the force propagation through the hydraulic medium, from the differential pressure source to the effective piston force, is weakened for higher frequencies and additionally lagged for a certain frequency range.

We recall that for the Zener model to be dissipative and, therefore, physically reasonable for real materials (correspondingly media), the thermodynamic constraints of the parameters $\alpha = \beta$ should be additionally satisfied, as has

been formerly observed in multiple rheological studies and also theoretically proved in [17].

The above physical constraints on the time-constants and differential-orders lead us to the four-parameters linear fractional-order model (17) of the viscoelastic hydraulic cylinders with negligible inertial terms.

3.3. Initial value and impulse response

Next we need clarifying the initial conditions for fractional differential equation (17). The initial condition for the integer-order dashpot, which is the relative displacement at $t = 0$, can be assumed zero without loss of generality. The remaining fractional-order dynamics of the Zener model requires the single initial condition ${}_0D_t^{\alpha-1}x(t)$, cf. [1], provided the input differential pressure, correspondingly actuation force, is a known exogenous value. It has been shown in [1] that for a physically reasonable (i.e. continuous) loading, or even in the case of a step discontinuity, zero initial conditions for the strain dynamics apply. Non-zero initial conditions will only be valid in case of a stress impulse $B \delta(t)$, then resulting in, cf. [1],

$$\left[\lambda_2 {}_0D_t^{\alpha-1}x(t) \right]_{t \rightarrow 0} = B. \quad (18)$$

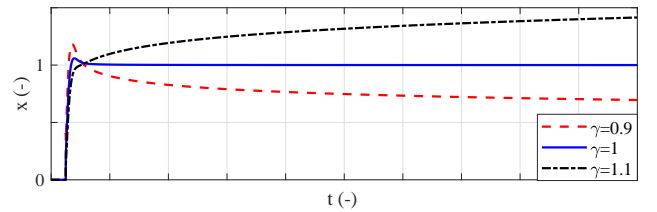


Figure 2: Impulse response for various order $\gamma = \{0.9, 1, 1.1\}$.

We have now to perform a closer look on the impulse response of (17), and that in terms of the final value problem from which the $\gamma = 1$ constraint is enlightened. Rewriting (17) in the time domain and integrating both sides with respect to dt^γ results in

$$\mu \lambda_2 {}_0D_t^\alpha x(t) + \mu x(t) = {}_0D_t^{-\gamma} (\lambda_1 {}_0D_t^\beta \tau(t) + \tau(t)). \quad (19)$$

Since $\alpha, \beta > 0$ both differential terms vanish for $t \rightarrow \infty$ and solving, this way, the final value problem yields

$$[x(t)]_{t \rightarrow \infty} = \mu^{-1} \int_0^t \tau(t) dt^\gamma. \quad (20)$$

For the applied Dirac impulse $\delta(t)$ the integral solution (20) can be directly evaluated, given (see e.g. [15])

$${}_0D_t^\eta \delta(t) = \frac{t^{-\eta-1}}{\Gamma(-\eta)}. \quad (21)$$

It can be shown that for $\eta < 0$ the value of (21) remains $\forall t > 0$ constant and equal to one for $\eta = -1$ only. Otherwise it converges to zero for $-1 < \eta < 0$ and diverges for

$\eta < -1$. For the final value (20), it means that a constant non-zero impulse response of the relative displacement can only be achieved when $\gamma = 1$. Indeed the free integrator in (17) requires a constant finite displacement as result of a force impulse which has finite energy content. An illustrative numerical example of the (17) model response to the input impulse is shown in Figure 2 for $\gamma = \{0.9, 1, 1.1\}$.

4. Experimental evaluation and discussion

The experimental evaluation of the above model was made with the data recorded from a standard linear-stroke hydraulic cylinder in laboratory setting. More details on the experimental setup can be found in [18]. The relative displacement $x(t)$ is directly measured by a linear encoder while the differential pressure $\tau(t)$ is obtained from two pressure sensors installed on each of the cylinder chambers.

4.1. Frequency response function

The measured frequency response function $G(j\omega) = x(j\omega)/\tau(j\omega)$ is used for the least-squares fit of the fractional-order model (17). Note that both, the amplitude response in dB and phase response in deg have been equally incorporated into the objective function. For the sake of comparison, the least-squares best fit has been found, from the same experimental data, also for the integer-order model with the structure as in (17). The measured and both ways modeled frequency response function are shown opposite to each other in Figure 3. The fractional-order model coincides with the measurements while the integer-order one misses the phase response.

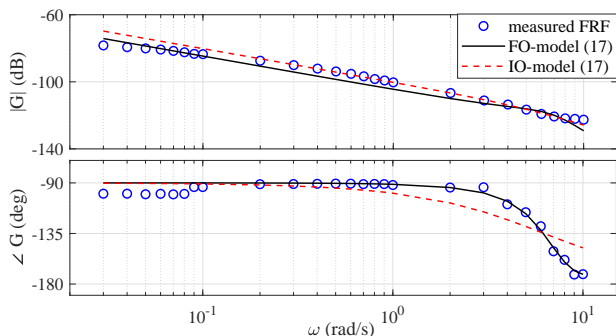


Figure 3: Measured and (17)-modeled frequency response function; least-squares best fit for fraction- and integer-order derivatives.

4.2. Time series

Similar observation is when comparing the time series of the identified fractional- and integer-order models with the initial phase of the measured response to the slope-shaped input $\tau(t)$. From Figure 4, one can see that only the fractional-order model captures a lagged transient of the relative displacement. Note that further progress (not shown in the figure) diverge from each other in all cases, due to an inherent integration error. Yet the fractional-order model reproduces the initial transition of the viscoelastic response to a linearly increasing input force.

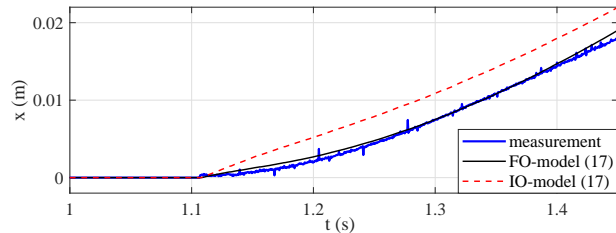


Figure 4: Measured and (17)-modeled time response to slope input.

Acknowledgment

This research received funding from IS-DAAD program under RCN project number 294835. Laboratory measurements performed by Daniela Kapp are also acknowledged.

References

- [1] N. Heymans, I. Podlubny, Physical interpretation of initial conditions for fractional differential equations with riemannliouville fractional derivatives, *Rheol. Acta* 45 (2006) 765–771.
- [2] F. Mainardi, G. Spada, Creep, relaxation and viscosity properties for basic fractional models in rheology, *The European Physical Journal Special Topics* 193 (1) (2011) 133–160.
- [3] M. Caputo, F. Mainardi, A new dissipation model based on memory mechanism, *Pure and App. Geop.* 91 (1971) 134–147.
- [4] F. Meral, T. Royston, R. Magin, Fractional calculus in viscoelasticity: an experimental study, *Communications in Nonlinear Science and Numerical Simulation* 15 (4) (2010) 939–945.
- [5] C. Ionescu, A. Lopes, D. Copot, J. T. Machado, J. Bates, The role of fractional calculus in modeling biological phenomena: A review, *Communications in Nonlinear Science and Numerical Simulation* 51 (2017) 141–159.
- [6] J. T. Machado, Fractional order modelling of dynamic backlash, *Mechatronics* 23 (7) (2013) 741–745.
- [7] Y. Liu, J. Shan, N. Qi, Creep modeling and identification for piezoelectric actuators based on fractional-order system, *Mechatronics* 23 (7) (2013) 840–847.
- [8] T. J. Freeborn, B. Maundy, A. S. Elwakil, Measurement of supercapacitor fractional-order model parameters from voltage-excited step response, *IEEE Journal on Emerging and Selected Topics in Circuits and Systems* 3 (3) (2013) 367–376.
- [9] C. A. Monje, B. M. Vinagre, V. Feliu, Y. Chen, Tuning and auto-tuning of fractional order controllers for industry applications, *Control engineering practice* 16 (7) (2008) 798–812.
- [10] P. Shah, S. Agashe, Review of fractional PID controller, *Mechatronics* 38 (2016) 29–41.
- [11] D. D. Joseph, *Fluid Dynamics of Viscoelastic Liquids*, Springer, 1990.
- [12] M. Jelali, A. Kroll, *Hydraulic servo-systems: modelling, identification and control*, Springer, 2012.
- [13] K. Oldham, J. Spanier, *The fractional calculus theory and applications of differentiation and integration to arbitrary order*, Elsevier, 1974.
- [14] S. G. Samko, A. A. Kilbas, O. I. Marichev, et al., *Fractional integrals and derivatives*, Gordon and Breach Science, 1993.
- [15] I. Podlubny, *Fractional differential equations*, Elsevier, 1998.
- [16] D. Y. Song, T. Q. Jiang, Study on the constitutive equation with fractional derivative for the viscoelastic fluids—modified Jeffreys model and its application, *Rheol. Acta* 37 (1998) 512–517.
- [17] R. L. Bagley, P. J. Torvik, On the fractional calculus model of viscoelastic behavior, *J. of Rheology* 30 (1986) 133–155.
- [18] P. Pasolli, M. Ruderman, Linearized piecewise affine in control and states hydraulic system: Modeling and identification, in: *IEEE 44th Annual Conference of the Industrial Electronics Society*, 2018, pp. 4537–4544.